Exome sequencing links the SUMO protease SENP7 with fatal arthrogryposis multiplex congenita, early respiratory failure and neutropenia

Samra, N.; Jansen, N.S.; Morani, I.; Kakun, R.R.; Zaid, R.; Paperna, T.; ... ; Weiss, K.

Original research

Exome sequencing links the SUMO protease SENP7 with fatal arthrogryposis multiplex congenita, early respiratory failure and neutropenia

Nadra Samra,[1,2] Nicolette S Jansen,[3] Ilham Morani,[1] Reli Rachel Kakun,[4] Rinat Zaid,[5] Tamar Paperna,[5] Mario Garcia-Dominguez,[6] Yuri Viner,[2,7] Hilel Frankenthal,[2,7] Eric S Shinwell,[2,8] Igor Portnov,[2,8] Doua Bakry,[2,9] Adel Shalata,[10] Mika Shapira Rootman,[11] Dvora Kidron,[12] Laura A Claessens,[3] Ron A Wevers,[13] Hanna Mandel,[14] Alfred C O Vertegaal [ID],[3] Karin Weiss [ID] [5,15]

ABSTRACT

Background SUMOylation involves the attachment of small ubiquitin-like modifier (SUMO) proteins to specific lysine residues on thousands of substrates with target-specific effects on protein function. Sentrin-specific proteases (SENPs) are proteins involved in the maturation and deconjugation of SUMO. Specifically, SENP7 is responsible for processing polySUMO chains on targeted substrates including the heterochromatin protein 1α (HP1α).

Methods We performed exome sequencing and segregation studies in a family with several infants presenting with an unidentified syndrome. RNA and protein expression studies were performed in fibroblasts available from one subject.

Results We identified a kindred with four affected subjects presenting with a spectrum of findings including congenital arthrogryposis, no achievement of developmental milestones, early respiratory failure, neutropenia and recurrent infections. All died within four months after birth. Exome sequencing identified a homozygous stop gain variant in *SENP7* c.1474C>T; p.(Gln492*) as the probable aetiology. The proband's fibroblasts demonstrated decreased mRNA expression. Protein expression studies showed significant protein dysregulation in total cell lysates and in the chromatin fraction. We found that HP1α levels as well as different histones and H3K9me3 were reduced in patient fibroblasts. These results support previous studies showing interaction between SENP7 and HP1α, and suggest loss of SENP7 leads to reduced heterochromatin condensation and subsequent aberrant gene expression.

Conclusion Our results suggest a critical role for SENP7 in nervous system development, haematopoiesis and immune function in humans.

WHAT IS ALREADY KNOWN ON THIS TOPIC

⇒ Abnormalities in protein SUMOylation were linked with various human diseases; however, knowledge on the specific roles of the SUMOylation machinery is limited.

WHAT THIS STUDY ADDS

⇒ In this study, we demonstrate a homozygous loss-of-function variant in SENP7, encoding a small ubiquitin-like modifier protease, is associated with fatal arthrogryposis, respiratory failure and neutropenia.

HOW THIS STUDY MIGHT AFFECT RESEARCH, PRACTICE OR POLICY

⇒ Our results support a critical role for SENP7 in nervous system development and immune function in humans.

INTRODUCTION

Virtually all cellular processes are tightly regulated by post-translational modifications (PTMs). PTMs involve enzyme-mediated covalent addition of functional groups to proteins during or after synthesis. PTMs are reversible; dedicated enzymes can remove PTMs. These modifications greatly increase the complexity of functional proteomes.[1] SUMOylation is a key PTM that involves the covalent attachment of small ubiquitin-like modifier (SUMO) proteins to specific lysine residues on thousands of substrates, regulating protein stability, solubility, localisation, protein interactions and other processes.[2]

The mammalian SUMO family consists of at least four members, SUMO 1–4. The SUMO conjugation cascade is similar to the ubiquitylation cascade, involving three main steps: E1 (activating), E2 (conjugating) and E3 (ligating)[3 4] (figure 1). SUMOylation homeostasis is achieved via sentrin-specific proteases (SENPs) that are involved in maturation and deconjugation of SUMO.[3 5] SENP6 and SENP7 are dedicated SUMO proteases responsible for processing polySUMO chains on targeted substrates as their catalytic domains differ from other SENP family members. SENP6 has been affiliated with centromere-associated proteins, while SENP7 is affiliated with chromatin-associated proteins.[6–9] The crystal structure of SENP7 has revealed a unique loop insertion present in the catalytic domain,[10] giving it a specific point of contact for interaction with the SUMO2 isoform.[11]

An increasing number of studies provide evidence that abnormalities in SUMO regulation are associated with human diseases,[2 12] including
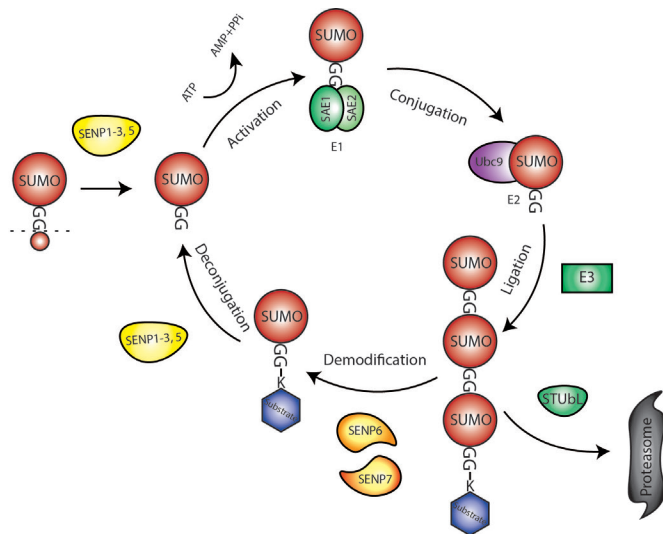
Figure 1 SUMOylation cycle. Overview of the conjugation and subsequent deconjugation of small ubiquitin-like modifier (SUMO) (depicted in red) on substrates facilitated by E1 (SAE1/SAE2), E2 (UBC9) and E3 enzymes. The polySUMO chain can be subsequently disassembled by sentrin-specific proteases (SENP)6 and SENP7 and ultimately deconjugated from the substrate by SENP1–3, 5.

cancer,[13] cardiac disease[14–16] and neurodegenerative disorders.[17] Furthermore, few components of the SUMO pathway have been previously shown to be associated with Mendelian disease. For instance, *RANBP2* which encodes a SUMO E3 ligase has been associated with autosomal dominant susceptibility to acute infection-induced encephalopathy,[18] and heterozygous pathogenic variants in SUMO-activating enzyme subunit 2 cause aplasia cutis congenita with ectrodactyly skeletal syndrome.[19] However, there are no previous reports on the association between SUMO proteases and human disease.

Here, we describe four subjects from a large consanguineous family with a novel fatal multisystemic syndrome caused by a homozygous stop-gain variant in *SENP7*. The clinical features include fetal akinesia syndrome, arthrogryposis multiplex congenita (AMC), congenital neutropenia, severe infections, no achievement of developmental milestones, early respiratory failure and death. Proteomic studies in the proband's cells identify multiple dysregulated proteins including proteins related to epigenetic regulation and chromosome organisation, including reduced levels of heterochromatin protein 1α (HP1α), a known SENP7 target. Overall, our study demonstrates altered protein expression in cells lacking functional SENP7, causing disrupted central nervous system (CNS) development and immune function leading to early death.

METHODS
Subjects
The extended family was evaluated by several metabolic and clinical genetics specialists at Ziv Medical Center since 2009. Exome sequencing (ES) was performed on the last patient born in 2021, prompting segregation studies in DNA samples of previously affected family members and healthy relatives. We reviewed the medical records, labs, imaging and autopsy findings when available of four affected subjects.

Exome sequencing
Following informed consent, clinical ES was performed on DNA extracted from peripheral blood in Hadassah Medical Center, Jerusalem. Exonic sequences were enriched using IDT xGen Exome Research Panel V.2 (Integrated DNA Technologies, Iowa, USA). Sequences were determined by Novaseq 6000 (Illumina, San Diego, California, USA) as 150 bp paired-end reads. Data analysis including read alignment and variant calling was performed with DNAnexus software (Palo Alto, California, USA) using default parameters, with the human genome assembly hg19/GRCh37 as reference. Variants were filtered out if the total read depth was <8X, if they were off-target (>8 bp from splice junction), synonymous or if the minor allele frequency was 0.01 in the Genome Aggregation Database (gnomAD) or Hadassah in-house exome database.

Sanger segregation
Each predicted disease-causing variant was confirmed by Sanger sequencing according to standard methods, and co-segregation analysis was performed in the rest of the family members' DNA samples. Primers used to amplify the variant-containing regions are detailed in the online supplemental file 1.

Co-segregation evidence calculation
Co-segregation evidence was calculated based on the probability of segregation results of a fully penetrant recessive disorder in each family member similar to what was described by Javrik and Browning.[20] For example, the probability of an affected sibling being a homozygous mutant is 1/4, and the probability of an unaffected sibling being either homozygous wild type or carrier is 3/4.

Tissue culture and fibroblasts
SK47 (patient III-4 fibroblasts) were cultured in Dulbecco's modified Eagle's medium (DMEM) (high glucose, pyruvate, Gibco) supplemented with 10% fetal bovine serum and 100 U/mL penicillin and 100 µg/mL streptomycin (Gibco). Control fibroblasts FSE-hTERT (immortalised fibroblasts from a male baby foreskin) and un-hTERT (immortalised fibroblasts from a male baby) were grown under similar conditions as patient fibroblasts.[21]

RNA studies
RNA was extracted using the PureLink RNA Mini Kit (12183018, Thermo Fisher); 1.5 µg of total RNA was used as a template for cDNA synthesis using High Capacity cDNA Reverse Transcription Kit (4368814, Thermo Fisher). cDNA amplification of exons 1–4 proximal to stop gain variant was performed in the patient fibroblasts and control using GoTaq Green Master Mix (M7122, Promega) and SENP7 primers detailed in the online supplemental file 1.

qPCR was performed to evaluate SENP7 mRNA levels using Fast SYBR Green Master Mix (4385612, Thermo Fisher). The reaction was performed using 0.2 µM of SENP7-specific primers and 20 ng of cDNA as a template using QuantStudio3 qPCR machine. *GAPDH* mRNA levels were used for normalisation.

Proteomics studies
Total protein lysates and chromatin fractions were prepared as previously described with minor changes[7] and analysed with an Exploris 480 mass spectrometer (Thermo Fisher Scientific, Bremen, Germany). For further details, see online supplemental file 3 and online supplemental file 4. For both the analysis of the total lysate samples and the chromatin fraction, four biological replicates per cell line were processed and analysed. All raw data

were analysed using MaxQuant software V.2.1.3.0 using search engine Andromeda.[22]

For the identification of proteins in the chromatin and total lysate samples of the patient fibroblasts, the MaxQuant output table 'protein groups' was uploaded into Perseus V.1.6.14.0 and V.2.0.7.0.[23] First, potential incorrect identified proteins were filtered out by 'only identified by site', 'reverse' and 'potential contaminant'. LFQ scores were then transformed to log2 scale and replicates of the same cells were grouped. Data were further filtered, requiring that the values should be valid and found in all four replicates within one group. Missing values were replaced by values from the total data matrix's normal distribution with a width of 0.3 and a downshift of 1.8. Control cell lines were then grouped as biological replicates and two-sample t-tests were performed. Targets were selected by having a −log10 p value of >1.3 (p<0.05) and an LFQ intensity difference of at least one on the log2 scale. The mass spectrometry proteomics data have been deposited to the ProteomeXchange Consortium via the PRIDE partner repository with the dataset identifier PXD040206.[24]

shRNA-mediated SENP7 knockdown

For shRNA-mediated knockdown, third-generation lentivirus was produced by transfecting HEK 293T cells with lentiviral packaging plasmids and plasmids containing SENP7 or non-targeting control shRNA. Plasmids for lentiviral production of shRNA targeting SENP7 are listed in the online supplemental file 1. Viruses were harvested in DMEM and titres were determined by ELISA. Cells were infected with a multiplicity of infection of three. Infection was performed in DMEM containing 8 µg/mL polybrene and medium was replaced after 24 hours. Cells were harvested and lysed three days postinfection.

Western blot analysis

Proteins were separated according to molecular weight on either precast 4%–12% Bis-Tris (Bolt, Thermo Fisher Scientific) or precast 3%–8% Tris-Acetate gels (NuPage, Thermo Fisher Scientific). Proteins were transferred to 0.45 µm nitrocellulose Amersham Protran Premium membrane (Sigma-Aldrich) using a submarine system. For the visualisation of total protein content, membranes were stained with Ponceau S (Sigma-Aldrich, P7170). Membranes were blocked with 8% milk powder in 1× phosphate-buffered saline containing 0.05% Tween-20 and subsequently incubated with primary antibody (online supplemental file 1) overnight on a rotating system at 4°C. Membranes were incubated with either donkey antirabbit IgG-HRP or goat antimouse IgG-HRP secondary antibodies in 1:5000 dilution in 8% milk. Antibodies were detected with Clarity (Max) Western ECL substrate (Bio-Rad, 170-5060, 170-5062) and captured with the iBright CL1500 Imaging System (Invitrogen).

RESULTS
Case descriptions

The proband, III-4 (figure 2A, table 1) was a male baby born after an uneventful pregnancy at 34-week gestation via caesarean section (CS) due to breech presentation and acute fetal distress. Apgar score was 5 at 1' and 7 at 5'. After birth, he was hypotonic with shallow breathing and required nasal continuous positive airway pressure (CPAP). Physical examination showed arthrogryposis of large and small joints. He had severe neutropenia—0.0 neutrophils, documented on his first day of life with no evidence of alloimmune neutropenia. It continued until granulocyte colony-stimulating factor (G-CSF) treatment was

commenced with an increase in neutrophil counts (online supplemental table 1S). Bone marrow aspirate showed myeloid maturation arrest (figure 2B). Brain MRI showed delayed myelination and symmetric white matter hyperintensities in the basal ganglia and periventricular area (figure 2C). During the admission, he was diagnosed with necrotising enterocolitis. Stool cultures and PCR for cytomegalovirus (CMV) were negative. A gene panel for congenital neutropenia was non-diagnostic. A follow-up physical examination revealed shallow breathing, truncal hypotonia, scarce spontaneous movements, with increased muscle tone and clonus of the limbs. There was mild eyelid and limb oedema. After the infant was discharged home, he had an aspiration episode which led to cardiorespiratory arrest. He was resuscitated at home and re-admitted. Bilateral bronchopneumonia was documented on chest X-ray. A respiratory viral panel was positive for adenovirus. In the intensive care unit (ICU), due to ineffective breathing and pending respiratory failure, he was put on mechanical ventilation. Laboratory studies on admission revealed white blood cells; 5900 with 33.5% neutrophils (1970) (on 10 µg/kg G-CSF). Serum albumin was 2.2 and dropped to 1.6 g/dL. C reactive protein (CRP) was 24 (control: 0–5 mg/L). The infectious workup was negative. Cerebrospinal fluid (CSF) revealed elevated protein—97 (control 10–40 mg/dL) but no cells, glucose 56 mg/dL and negative cultures/viral PCRs. Three weeks following admission, his CRP increased to 200 mg/L, accompanied by an increase in procalcitonin. A week before death his abdomen became swollen and tender. Abdominal X-ray revealed marked dilatation of small and large intestinal loops with free fluid. Peritoneal puncture grew *Enterococcus faecalis*. Urine culture revealed *Candida albicans*. Despite broad antibiotics, his condition continued to deteriorate and he died several weeks later.

III-3 (figure 2A. table 1) was the younger sibling of the proband. The pregnancy was reported as normal including a fetal ultrasound at 26-week gestation. She was also born at 34 weeks via urgent CS due to breach presentation and fetal distress. Apgar score was 5 at 1' and 8 at 5'. Shortly after delivery, she presented with apnoea and bradycardia. Following a short resuscitation, she was put on CPAP for 12 hours. On physical examination, there was generalised arthrogryposis. The echocardiogram demonstrated a bicuspid aortic valve. She remained in the ICU for a month. At first, she was fed by nasogastric tube but gradually switched to bottle feeding. While seemingly gaining weight she also had oedema of eyelids, hands and feet. Her routine laboratory studies were normal including a complete blood count with no evidence of neutropenia, and normal kidney and liver function, except for a mild reduction of serum albumin—3.1 g/dL (normal control 3.7–4.4). After one month, she was discharged home and scheduled for follow-up studies which unfortunately was never accomplished. Several weeks later, she was found in her crib at home with cyanosis and cardiorespiratory arrest. Resuscitation failed.

III-7 was the first baby born in this kindred with AMC. He was born following an uneventful pregnancy. The mother reported normal prenatal ultrasound imaging, lastly performed at 26 weeks of gestation. He was delivered spontaneously, at week 42, Apgar score was 7 at 1' and 8 at 5'. He had a faint cry with shallow breathing and was treated with oxygen for 24 hours. Physical examination disclosed facial dysmorphism and severe AMC involving most of the big and small joints accompanied by truncal hypotonia and severe hypertonia and scissoring of lower limbs. During the first four days of life, he had difficulty sucking necessitating the insertion of a nasogastric tube, and gradually switching to bottle feeding. He was discharged home
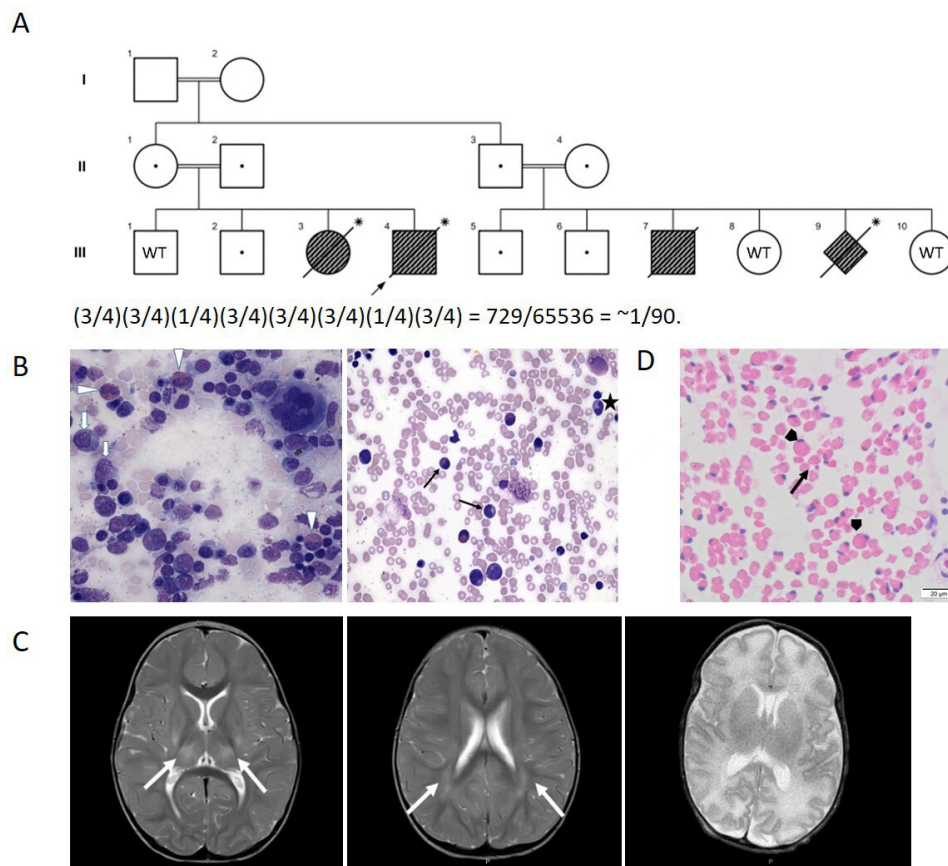
$$(3/4)(3/4)(1/4)(3/4)(3/4)(3/4)(1/4)(3/4) = 729/65536 = {\sim}1/90.$$

Figure 2 The sentrin-specific protease (SENP)7-related disorder. (A) A simplified pedigree of the family is shown. Note II-1 and II-2 are first cousins, and II-3 and II-4 are first cousins as well. Affected patients are marked in grey, asterisk marks the presence of the homozygous stop-gain variant p.(Gln492*) in *SENP7*. For III-7 a DNA sample was not available. All healthy family members were tested and were found to be a carrier of the SENP7 variant (central dot) or wild type (WT). Co-segregation evidence was calculated based on the result in each tested subject except for the proband and the parents in both sibships. For example, the probability III-3 is homozygous mutant is 1/4, the probably III-1 and III-2 are not homozygous mutant is $(3/4)^2$ and so on. (B) Bone marrow aspirate showing myeloid maturation arrest. Most of the myeloid cells present are either at the promyelocytic (white arrows), myelocytic (black arrows) or metamyelocytic (star) stages of maturation. There is a notable increase of erythroid and eosinophils precursors (arrow heads). Prominent lymphocytosis is seen. (C) Left image: axial T2-weighted (T2W) image at the level of the basal ganglia. Symmetrical foci of T2 hyperintensity are noted in the lentiform and thalami bilaterally (arrows). The ventricles are within normal limits. Middle image: axial T2W image at the level of the lateral ventricles. There are confluent areas of T2 hyperintensity at the periventricular and deep white matter in the biparietal region (arrows). Right image: axial T2W at the level of the basal ganglia. Myelination is delayed. (D) A psoas muscle transverse section. Variability in size of muscle fibres, hypertrophic fibres (arrow heads) alternating with thin atrophic fibres (arrows) (H&E).

and scheduled for future studies and follow-up, but the family did not return to follow-up. A month later, he was admitted to the ICU due to diarrhoea during the last three days and apnoeic episodes which started on the morning of his admission. Physical examination revealed an encephalopathic baby not responding to pain stimuli, featuring shallow breathing with a decrease in oxygen saturation. He had oedema of eyelids and pitting oedema of limbs. Umbilical and large right inguinal hernias were noted. He had failure to thrive weighing only 3040 g. Laboratory studies revealed severe neutropenia (online supplemental table 1S), CSF protein was mildly elevated at 87 mg/dL but no cells were found and bacterial culture was negative. Urine culture grew *Enterococcus* which was treated with antibiotics. Viral serology including respiratory syncytial virus and CMV were negative. Over the next few days, he continued to deteriorate necessitating mechanical ventilation but died of progressive respiratory failure.

III-9 was a fetus with ultra-sonographic findings of fetal akinesia at 30 weeks of gestation. These findings suggested that the fetus might suffer from the same disorder as his deceased brother III-7. On autopsy, a female fetus weighed 1295 g and appeared appropriate for gestational age. Facial dysmorphic features included hypertelorism, a flat nose and bilateral pes equinovarus. The combined weight of the lungs was 28 g, consistent with 28-week gestation, suggestive of early pulmonary hypoplasia. The weight of the brain was normal for gestational age. Histopathological studies revealed a normal cortex consisting of six well-organised layers. Furthermore, there was no evidence of a migration defect. The spinal cord appeared normal with well-appearing neurons in the anterior horn. The histological section of the psoas muscle revealed variability of muscle fibre diameter including hypertrophic fibres alternating with atrophic fibres suggestive of a neurogenic pattern (figure 2D).

Sequencing results and RNA studies

The proband underwent singleton ES that revealed homozygous loss-of-function variants in three genes not known to be associated with disease: *ABHD1*, *SENP7* and *TXNRD1*. Segregation was performed for all detected variants for two affected

Table 1 Main clinical features of affected infants

	III-4	III-3	III-7
Week gestation	34	34	42
Birth weight	1700 g (5%ile)	1560 g (4%ile)	2845 g (6%ile)
Birth head circumference	32 cm	30.5 cm	33.5 cm
Arthrogryposis	+ Elbows, wrists, fingers and hips	+ Hips, knees, elbows, wrists and fingers	+ Most large and small joints
Truncal hypotonia	+	+	+
Limb hypertonia/Clonus	+	+	+
Faint cry/Shallow breathing	+	+	+
Progressive oedema of eyelids and limbs	+	+	+
Neutropenia	+	−	+
Failure to thrive	+	+	+
Dysmorphic features	High forehead, wide-spaced eyes with ptosis of eyelid, low nasal bridge, long and deep philtrum, thin lips, full cheeks, myopathic faces with down turned mouth	Blepharophimosis, widespaced eyes, retrognathia, high arched palate, small thoracic cage	Wide spaced eyes, upturned wide nose, long and grooved philtrum, microretrognathia, low set ears and a high arched palate. Short neck, low posterior hairline and bilateral single palmar crease, short and narrow ribcage.

subjects (III-3, III-9) of whom a DNA sample was available, and the healthy parents and siblings (online supplemental table 2S). Only the *SENP7* variant segregated among all affected and unaffected family members as expected. The detected variant in *SENP7* (NM_020654.5): c.1474C>T; p.(Gln492*) is rare and not reported in general population databases such as gnomAD. The variant is in exon 10/24 and is predicted to create a truncated protein lacking the catalytic domain in the C-terminal end (figure 3A,B). cDNA generated from fibroblasts of III-4 compared with a control sample showed decreased mRNA levels in the affected sample, suggesting nonsense-mediated mRNA decay (figure 3C).

Protein expression studies

To elucidate the effect of truncated SENP7 on chromatin-affiliated proteins, fibroblasts belonging to proband III-4 and two comparable age control fibroblast cell lines were grown and fractionated using high sucrose concentration to obtain the chromatin fraction (figure 4A, online supplemental file 3). In total, 4148 proteins were identified by mass spectrometry. After

stringent filtering, where a minimum of four valid values had to be found in at least one experimental group, 2253 proteins remained (online supplemental file 3). One hundred forty-five proteins were identified to be significantly upregulated at least twofold and 161 proteins were identified to be significantly downregulated at least twofold in proband III-4 fibroblasts (figure 4B). Interestingly, among these targets were protein families relating to epigenetic regulation (highlighted in blue figure 4C), metabolic processes and cytoskeletal organisation (highlighted in red figure 4D), gene transcription and chromosome organisation (online supplemental file 3). Noteworthy, downregulation of various members of the histone family was observed in the patient cells (figure 4E). Interestingly, SUMOylated HP1α was previously identified as target for SENP7.[8][25] HP1α plays a key role in heterochromatin homeostasis, where it enables compaction of heterochromatin via H3K9me3 binding.[26][27] We did not detect HP1α in the chromatin fractions by mass spectrometry, but this could be due to its small size and its lysine-rich and arginine-rich regions that hamper identification by mass spectrometry. Therefore, we decided to verify HP1α
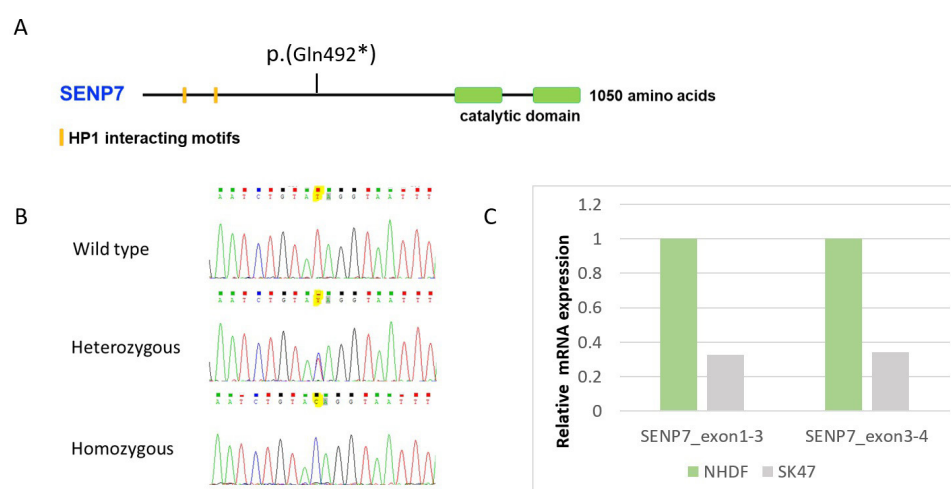
Figure 3 Truncating variant in sentrin-specific proteases (SENP)7 likely results in loss of function. (A) Diagram of long SENP7 isoform domain and the predicted truncated SENP7 protein due to p.(Gln492*) variant. (B) Sanger chromatogram showing wild-type, heterozygous carrier and homozygous sequence. (C) qPCR of RNA extracted from the patient's fibroblasts cells (SK47) and control fibroblasts (NHDF) showing >50% decrease in cDNA levels of exons 1–3 and exon 3-4.

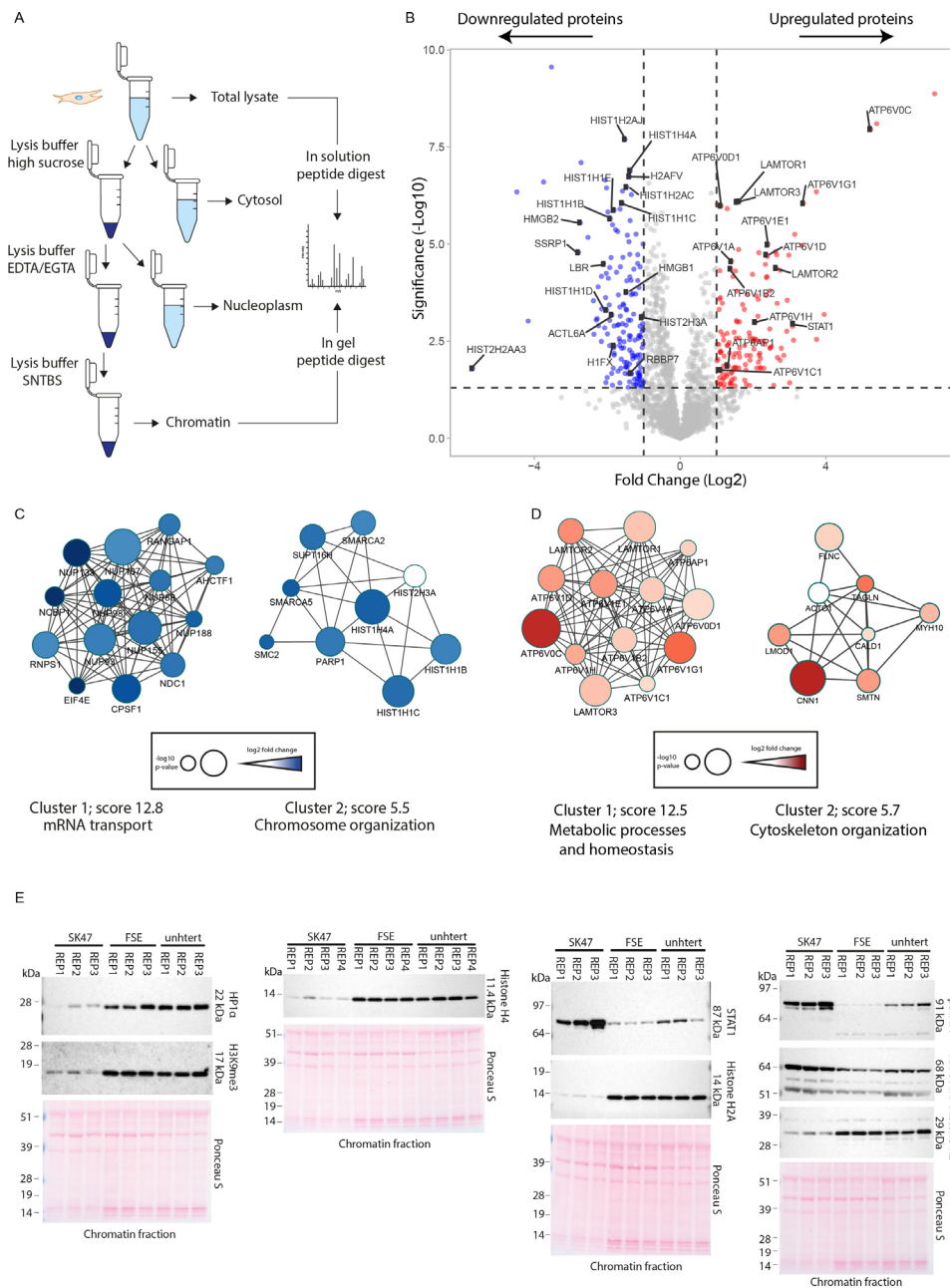**Figure 4** Truncated sentrin-specific proteases (SENP)7 potentially affects various cellular processes. (A) Experimental setup of the chromatin fractionation assay and subsequent chromatin and total lysate mass spectrometry. (B) Volcano plot of proteins identified in the chromatin fraction of the patient fibroblasts compared with the FSE-hTERT and un-hTERT control fibroblasts. The x-axis represents protein abundance (log2) while the y-axis represents a $-\log10$ of p value. N=4 independent experiments. Histone-related proteins are marked with blue labels while cellular metabolism proteins are marked with red labels. (C) Cytoscape software with plugin MCODE was used to determine the most highly interconnected protein clusters. Protein clusters with a STRING interaction confidence of 0.7 or higher are shown. Cluster 1 of the downregulated fraction, visualised in blue, shows proteins belonging to mRNA transport and cluster 2 shows proteins belonging to chromosome organisation. (D) Cluster 1 of the upregulated fraction, visualised in red, shows proteins belonging to metabolic processes and homeostasis and cluster 2 shows proteins belonging to muscle structure development. (E) Patient fibroblasts (SK47) and two control fibroblasts (FSE-hTERT and un-hTERT) chromatin fractions were immunoblotted to validate proteins identified by mass spectrometry. SK47 shows reduced abundance of HP1α, histone H3 lysine 9 trimethylation, histone H4, histone H1.2 and histone H2A, while there is an increase seen for STAT1, phosphorylated STAT1 and ATP6V1A.

by immunoblotting. Strikingly, we found that HP1α levels were significantly reduced in the chromatin fraction of the patient cells (figure 4E). Consistently, we noted a reduction in the levels of the heterochromatin histone mark H3K9me3 (figure 4E). Furthermore, we found a reduction in protein lamin B receptor that anchors heterochromatin to the inner nuclear membrane (figure 4B, online supplemental file 3).

To evaluate if protein biogenesis of specific proteins was perturbed, mass spectrometry of total lysate samples was also performed. In total, 5076 proteins were found. After stringent data filtering, where a minimum of four valid values had to be found in at least one group, 2782 proteins remained. One hundred twenty-two proteins were identified to be upregulated significantly at least twofold and 304 proteins were identified
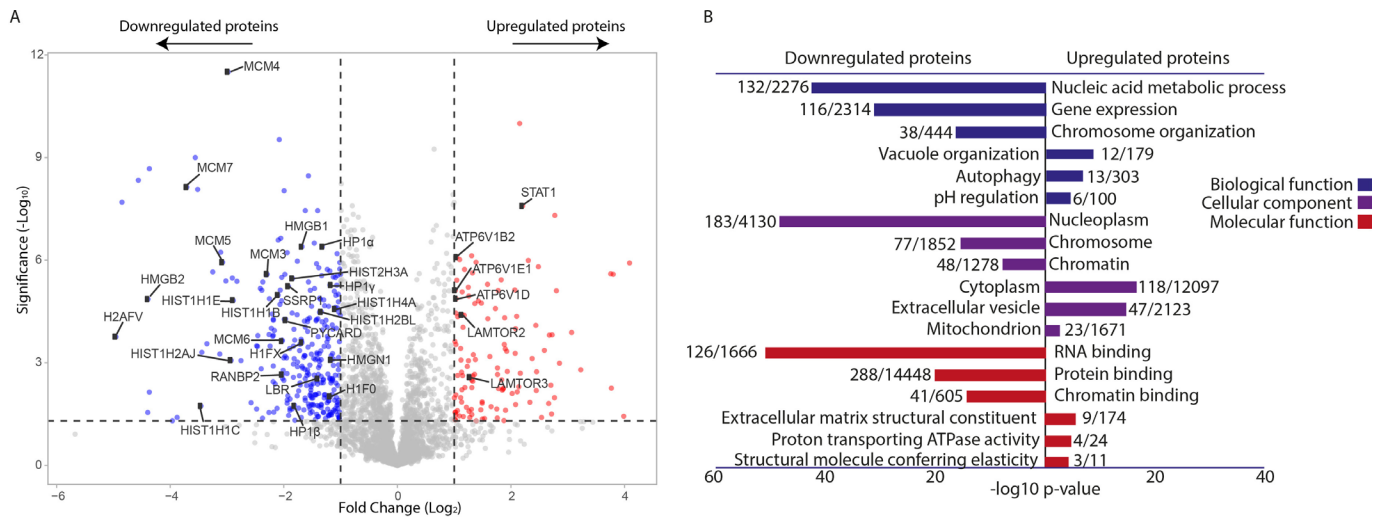
Figure 5 Patient cells are exhibiting affected proteins, mainly in the nucleus. (A) Volcano plot showing proteins identified by mass spectrometry in total cell lysates of patient cells compared with two control cell lines. The x-axis represents protein abundance (log2) while the y-axis represents a −log10 of p value. N=4 independent experiments. On the left side, downregulated proteins are displayed, histone proteins and MCM family members are highlighted in blue. On the right side, upregulated proteins are displayed, proteins belonging to cellular metabolism are highlighted in red. (B) Bar plot of data analysed by Gene Ontology (GO) representing downregulated proteins (log2 difference < −1) displayed on the left side and upregulated proteins (log2 difference >1) on the right side. GO terms for biological function, cellular component and molecular function are shown. Numbers belonging to bars indicate identified proteins versus proteins in the reference list that map to the particular data category. P value is calculated by Fisher's exact test and reflects the probability of random occurrence of genes in a category.

to be significantly downregulated at least twofold in patient fibroblasts (figure 5A). Proteins such as histones and HP1α (figure 5A) were found to be downregulated in both the chromatin fraction and in total lysates, indicating reduced protein biogenesis or reduced protein stability (online supplemental figure 3S). Interestingly, all three HP1 family members (HP1α, HP1β, HP1γ) were reduced in patient cells (figure 5A and online supplemental file 4). Gene Ontology analysis was performed on total proteome for biological functions, cellular components and molecular functions, showing reductions in nucleic acid metabolic processes, gene expression and chromosome organisation (figure 5B).

Knockdown of SENP7 in control cells
Furthermore, the question remained if SENP7 deficiency could lead to downregulation or upregulation of the same set of proteins as observed for truncated SENP7. An shRNA-mediated knockdown was performed on the two comparable age control fibroblast cell lines and total lysates were prepared 72 hours post-infection. However, no apparent change in total HP1α, STAT1, histone H1.2 and histone H4 protein levels in total lysates were found on acute loss of SENP7 (online supplemental figure 3S).

DISCUSSION
Here, we describe four subjects from a large consanguineous family with a novel fatal multisystemic syndrome. The clinical features include fetal akinesia syndrome, AMC, congenital neutropenia in two of three newborns, severe infections, no achievement of developmental milestones, early respiratory failure and death during infancy. Segregation studies in two patients, one aborted fetus and six healthy family members strongly support a homozygous loss-of-function variant in *SENP7* as disease-causing with co-segregation evidence of ~1/90 (figure 2A).[20]

SENP7 encodes a SENP protease, a member of the SUMO protease family.[5 28] Two SENP family members, SENP6 and

SENP7 are involved in disassembling polySUMO chains on targeted substrates.[29 30] Our findings indicate that SENP6 and SENP7 act non-redundantly since SENP6 is unable to compensate for the absence of SENP7. Therefore, it is likely that they regulate unique sets of substrates. Similar to other SENP proteins, SENP7 is widely expressed in various tissues and contains a C-terminal catalytic domain enabling its activity. Human SENP7 has two main isoforms.[29] The long isoform SENP7L is nuclear, whereas the shorter isoform SENP7S localises exclusively to the cytosol. SENP7L contains two tandem heterochromatin protein 1 (HP1) interacting motifs, found to contribute to locking of HP1α at pericentric heterochromatin.[25] The interaction of SENP7L with heterochromatin may affect embryonic development as well as tumourigenesis.[25]

The genetic basis of AMC is highly heterogeneous including genes encoding components required for the formation or the function of neuromuscular junctions, skeletal muscle, motor neurons, myelin of peripheral nerve, connective tissue or the central nervous system.[31] The patients we describe present with AMC and severe truncal hypotonia, combined with spasticity and clonus, likely due to central nervous system involvement. Brain MRI was performed in the proband and revealed delay in myelination at the level of the lateral ventricles and the basal ganglia. However, one cannot conclude whether it expresses hypomyelination or dysmyelination since both findings require follow-up imaging which is not available. Furthermore, symmetrical foci of T2 hyperintensity were noted in the lentiform nucleus and thalami bilaterally. Such a finding may suggest mitochondrial dysfunction. Notably, SUMOylation targeting mitochondrial-associated proteins is considered to regulate mitophagy activation and mitochondrial functions and dynamics.[32 33] The muscle biopsy of the aborted fetus was suggestive of neurogenic aetiology due to both hypertrophy and atrophy of muscle fibres. However, there might be primary muscular involvement too as SENP7 was shown to affect sarcomere organisation through regulation of *Myh1* gene transcription.[34] Interestingly,

there is previous preliminary evidence linking SENP7 and abnormal CNS development. One study showed SENP7 is upregulated during neuronal differentiation, and its knockdown compromised neurogenesis both in cell lines and embryos.[35] In addition, the international mouse phenotyping consortium[36] reports increased acoustic startle response and abnormal locomotor activity in Senp7tm1b(EUCOMM)Hmgu knockout mice, further supporting SENP7 involvement in neuronal development and potentially muscle development.

Another striking clinical finding was congenital neutropenia and severe infections documented in two out of three patients. There are no previous studies linking SENP7 with neutropenia, however, impaired SUMOylation resulted in abnormal hematopoietic progenitor cell development.[37 38] Furthermore, some key proteins involved in neutrophil maturation are SUMOylated, including C/EBP-γ and GFI1.[39 40] In our proteomics screen in fibroblasts, C/EBP-ζ was downregulated in patient cells, but we did not detect C/EBP-γ or GFI1. This might be due to cell-specific expression patterns. Interestingly, the clinical course of our patients may indicate a complex immune deficiency beyond neutropenia as G-CSF treatment did not prevent infections, and leukocytosis was not present during severe infections. Unfortunately, a full immunological workup including neutrophil and cellular function was not performed due to the severe and fatal clinical course. SENP7 was previously shown to regulate NLRP3 inflammasome activity and the nuclear factor kappa B pathway[41 42] and further studies are needed to determine whether the inflammasome pathway is involved in this condition.

As SENP7 is responsible for disassembling SUMO chains on targeted substrates, it may antagonise the SUMO-targeted ubiquitin ligase (STUbLs) pathway.[30] Therefore, we hypothesise that SENP7 inactivation might lead to accumulation of SUMO chains on substrates including HP1α, possibly leading to STUbL-mediated ubiquitylation and subsequent proteasomal degradation.[8] Furthermore, SENP7 has been proposed to promote chromatin relaxation for DNA repair.[9]

To test whether loss of functional SENP7 alters total levels of proteins and incorporation of proteins in chromatin, we evaluated protein expression differences in total lysate and chromatin fractions in the patient's cells and controls. Our results show a significant dysregulation of protein expression profiles at both levels with more downregulated than upregulated proteins. Interestingly, proteins that were downregulated in the patient's cells were predominantly found in the nucleoplasm and chromatin. These results may indicate a role for SENP7 in chromatin regulation by possibly influencing the SUMOylation of substrates mainly located in the nucleus as previously proposed.[8 9] Remarkably, the histone family had the most affected members in the patient cells, being downregulated on both chromatin as well as in total proteome. The four core components of the histone family, namely histones H2A, H2B, H3 and H4 and H2A variants H2A.X and H2A.Z and linker histone H1 (including its variants) were low in cells expressing the truncated SENP7 version. This might be related to enhanced SUMOylation of HP1α in the absence of functional SENP7. Consistently, we identified a reduction of HP1α in chromatin fractions of the patient cells and in total lysates and a loss in the heterochromatin mark H3K9me3, indicating loss of heterochromatin compaction. The limited availability of patient fibroblasts did prevent the purification and identification of SUMO substrates.

The proteomic results presented the question if a knockdown of SENP7 would directly influence overall histone levels and chromatin histone levels. However, a temporary knockdown of SENP7 on control fibroblasts did not affect histone biogenesis

or HP1α levels. This could hint at a role for SENP7 in early development that cannot be recapitulated by a temporary loss of SENP7 in our experimental system. Alternatively, truncated SENP7 could act in a dominant negative manner as we cannot rule out a residual activity of the N-terminal part of SENP7L that binds HP1α. Furthermore, it would have been interesting to use fibroblasts from healthy siblings and/or parents as controls in our proteomics experiments, but unfortunately, they were not available.

Other altered proteins that are worthwhile to note include the SUMO E3 ligase RANBP2 and the SUMO-regulated protein STAT1. RANBP2 was downregulated in the total proteome and STAT1 was upregulated in the chromatin fraction as well as in the total proteome. On being stimulated by interferons (IFNs), phosphorylated STAT1 acts as a transcription factor and plays a key role in the immune response against viruses and mycobacteria.[43] Interestingly, our patient cells exhibited upregulation of STAT1 and an increased level of phosphorylated STAT1, indicating activation of IFN signalling in the absence of functional SENP7. More research is needed for mechanistic understanding of the link between a truncated version of SENP7 with immune signalling by STAT1 and the fatal disease phenotypes observed in patients.

In summary, we describe a novel disorder secondary to loss of SUMO protease SENP7, featuring fetal akinesia, AMC, early respiratory failure, no acquisition of developmental milestones, neutropenia and severe infections. Our results uncover critical possible novel roles for SENP7 in nervous system development (central and peripheral), haematopoiesis and immune function in humans.

Author affiliations
[1]Department of Genetics, Ziv Medical Center, Safed, Israel
[2]Azrieli Faculty of Medicine, Bar-Ilan University, Safed, Israel
[3]Department of Cell and Chemical Biology, Leiden University Medical Center, Leiden, The Netherlands
[4]The Clinical Research Institute, Rambam Health Care Campus, Haifa, Israel
[5]The Genetics Institute, Rambam Health Care Campus, Haifa, Israel
[6]Andalusian Centre for Molecular Biology and Regenerative Medicine-CABIMER, CSIC-Universidad Pablo de Olavide, Sevilla, Spain
[7]Pediatric Intensive Care Unit, Ziv Medical Center, Safed, Israel
[8]Department of Neonatology, Ziv Medical Center, Safed, Israel
[9]Department of Pediatric Hematology, Ziv Medical Center, Safed, Israel
[10]Simon Winter Institute for Human Genetics, Bnai Zion Medical Center, Haifa, Israel
[11]Department of Radiology, Rambam Health Care Campus, Haifa, Israel
[12]Department of Pathology, Meir Medical Center, Kfar Saba, Israel
[13]Translational Metabolic Laboratory, Department Laboratory Medicine, Radboud University Medical Centre, Nijmegen, The Netherlands
[14]Metabolic unit, Ziv Medical Center, Safed, Israel
[15]The Ruth and Bruce Rappaport Faculty of Medicine, Technion Israel Institute of Technology, Haifa, Israel

Ethics approval This study was approved by the Ziv Medical Center Helsinki Committee (study number 0089-17-ZIV) and the family consented to the publication of clinical data without photos.

Provenance and peer review Not commissioned; externally peer reviewed.

Data availability statement Data are available in a public, open access repository. Data are available on reasonable request. Additional raw data are available on request.

Supplemental material This content has been supplied by the author(s). It has not been vetted by BMJ Publishing Group Limited (BMJ) and may not have been peer-reviewed. Any opinions or recommendations discussed are solely those of the author(s) and are not endorsed by BMJ. BMJ disclaims all liability and responsibility arising from any reliance placed on the content. Where the content includes any translated material, BMJ does not warrant the accuracy and reliability of the translations (including but not limited to local regulations, clinical guidelines, terminology, drug names and drug dosages), and is not responsible for any error and/or omissions arising from translation and adaptation or otherwise.

ORCID iDs
Alfred C O Vertegaal http://orcid.org/0000-0002-7989-0493
Karin Weiss http://orcid.org/0000-0003-0998-810X

REFERENCES

1 Chen L, Kashina A. Post-translational modifications of the protein termini. *Front Cell Dev Biol* 2021;9:1–14.
2 Vertegaal ACO. Signalling mechanisms and cellular functions of SUMO. *Nat Rev Mol Cell Biol* 2022;23:715–31.
3 Celen AB, Sahin U. Sumoylation on its 25th anniversary: mechanisms, pathology, and emerging concepts. *FEBS J* 2020;287:3110–40.
4 Pichler A, Fatouros C, Lee H, *et al*. SUMO conjugation - a mechanistic view. *Biomol Concepts* 2017;8:13–36.
5 Nayak A, Müller S. SUMO-specific proteases/isopeptidases: SENPs and beyond. *Genome Biol* 2014;15:422.
6 Mukhopadhyay D, Arnaoutov A, Dasso M. The SUMO protease SENP6 is essential for inner kinetochore assembly. *J Cell Biol* 2010;188:681–92.
7 Liebelt F, Jansen NS, Kumar S, *et al*. The poly-SUMO2/3 protease SENP6 enables assembly of the constitutive centromere-associated network by group deSUMOylation. *Nat Commun* 2019;10:3987.
8 Maison C, Romeo K, Bailly D, *et al*. The SUMO protease SENP7 is a critical component to ensure HP1 enrichment at pericentric heterochromatin. *Nat Struct Mol Biol* 2012;19:458–60.
9 Garvin AJ, Densham RM, Blair-Reid SA, *et al*. The deSUMOylase SENP7 promotes chromatin relaxation for homologous recombination DNA repair. *EMBO Rep* 2013;14:975–83.
10 Lima CD, Reverter D. Structure of the human SENP7 catalytic domain and poly-SUMO deconjugation activities for SENP6 and SENP7. *J Biol Chem* 2008;283:32045–55.
11 Li Y, De Bolòs A, Amador V, *et al*. Structural basis for the SUMO2 isoform specificity of SENP7. *J Mol Biol* 2022;434:167875.
12 Yang Y, He Y, Wang X, *et al*. Protein SUMOylation modification and its associations with disease. *Open Biol* 2017;7:170167.
13 Seeler JS, Dejean A. SUMO and the robustness of cancer. *Nat Rev Cancer* 2017;17:184–97.
14 Liu Y, Zhao D, Qiu F, *et al*. Manipulating PML SUMOylation via silencing UBC9 and RNF4 regulates cardiac fibrosis. *Molecular Therapy* 2017;25:666–78.
15 Hotz PW, Müller S, Mendler L. SUMO-specific Isopeptidases tuning cardiac SUMOylation in health and disease. *Front Mol Biosci* 2021;8:786136.
16 Liang M, Cai Z, Jiang Y, *et al*. SENP2 promotes VSMC phenotypic switching via myocardin de-SUMOylation. *Int J Mol Sci* 2022;23:12637.
17 Mun M-J, Kim J-H, Choi J-Y, *et al*. Polymorphisms of small ubiquitin-related modifier genes are associated with risk of Alzheimer's disease in Korean: a case-control study. *J Neurol Sci* 2016;364:122–7.
18 Palazzo AF, Joseph J, Lim M, *et al*. Workshop on RanBP2/Nup358 and acute necrotizing encephalopathy. *Nucleus* 2022;13:154–69.
19 Schnur RE, Yousaf S, Liu J, *et al*. UBA2 variants underlie a recognizable syndrome with variable aplasia cutis congenita and ectrodactyly. *Genetics in Medicine* 2021;23:1624–35.
20 Jarvik GP, Browning BL. Consideration of cosegregation in the pathogenicity classification of genomic variants. *Am J Hum Genet* 2016;98:1077–81.
21 Samra N, Toubiana S, Yttervik H, *et al*. RBL2 bi-allelic truncating variants cause severe motor and cognitive impairment without evidence for abnormalities in DNA methylation or telomeric function. *J Hum Genet* 2021;66:1101–12.
22 Tyanova S, Temu T, Cox J. The MaxQuant computational platform for mass spectrometry-based shotgun proteomics. *Nat Protoc* 2016;11:2301–19.
23 Tyanova S, Temu T, Sinitcyn P, *et al*. The Perseus computational platform for comprehensive analysis of (prote)omics data. *Nat Methods* 2016;13:731–40.
24 Samra N, Jansen NS, Morani I, *et al*. Data from: exome sequencing links the SUMO protease Senp7 with fatal arthrogryposis multiplex congenita, early respiratory failure, and neutropenia. PRIDE repository. Available: https://www.ebi.ac.uk/pride/archive/projects/PXD040206/ [ ].
25 Romeo K, Louault Y, Cantaloube S, *et al*. The SENP7 SUMO-protease presents a module of two HP1 interaction motifs that locks HP1 protein at pericentric heterochromatin. *Cell Rep* 2015;10:771–82.
26 Bannister AJ, Zegerman P, Partridge JF, *et al*. Selective recognition of methylated lysine 9 on histone H3 by the HP1 chromo domain. *Nature* 2001;410:120–4.
27 Lachner M, O'Carroll D, Rea S, *et al*. Methylation of histone H3 lysine 9 creates a binding site for HP1 proteins. *Nature* 2001;410:116–20.
28 Talamillo A, Barroso-Gomila O, Giordano I, *et al*. The role of SUMOylation during development. *Biochem Soc Trans* 2020;48:463–78.
29 Kunz K, Piller T, Müller S. SUMO-specific proteases and isopeptidases of the SENP family at a glance. *J Cell Sci* 2018;131:jcs211904.
30 Jansen NS, Vertegaal ACO. A chain of events: regulating target proteins by SUMO polymers. *Trends Biochem Sci* 2021;46:113–23.
31 Kiefer J, Hall JG. Gene ontology analysis of arthrogryposis (multiple congenital contractures). *Am J Med Genet C Semin Med Genet* 2019;181:310–26.
32 Xiao H, Zhou H, Zeng G, *et al*. Sumoylation targeting mitophagy in cardiovascular diseases. *J Mol Med (Berl)* 2022;100:1511–38.
33 Huang C-J, Wu D, Khan FA, *et al*. Desumoylation: an important therapeutic target and protein regulatory event. *DNA Cell Biol* 2015;34:652–60.
34 Amrute-Nayak M, Gand LV, Khan B, *et al*. Senp7 deSUMOylase-governed transcriptional program coordinates sarcomere assembly and is targeted in muscle atrophy. *Cell Rep* 2022;41:111702.
35 Juarez-Vicente F, Luna-Pelaez N, Garcia-Dominguez M. The SUMO protease SENP7 is required for proper neuronal differentiation. *Biochim Biophys Acta* 2016;1863:1490–8.
36 Mouse Pheno type. n.d. Available: www.mousephenotype.org
37 Edrees MAH, Luo J, Sun F, *et al*. UBC9 deficiency selectively impairs the functionality of common lymphoid progenitors (CLPs) during bone marrow hematopoiesis. *Mol Immunol* 2019;114:314–22.
38 Yuan H, Zhang T, Liu X, *et al*. Sumoylation of CCAAT/enhancer-binding protein A is implicated in hematopoietic stem/progenitor cell development through regulating runx1 in zebrafish. *Sci Rep* 2015;5:9011.
39 Andrade D, Velinder M, Singer J, *et al*. Sumoylation regulates growth factor independence 1 in transcriptional control and hematopoiesis. *Mol Cell Biol* 2016;36:1438–50.
40 Bartels M, Govers AM, Fleskens V, *et al*. Acetylation of C/EBPε is a prerequisite for terminal neutrophil differentiation. *Blood* 2015;125:1782–92.
41 Barry R, John SW, Liccardi G, *et al*. SUMO-mediated regulation of NLRP3 modulates inflammasome activity. *Nat Commun* 2018;9:3001.
42 Li X, Jiao F, Hong J, *et al*. Senp7 knockdown inhibited pyroptosis and NF-ΚB/NLRP3 inflammasome pathway activation in raw 264.7 cells. *Sci Rep* 2020;10:1–7.
43 Tolomeo M, Cavalli A, Cascio A. STAT1 and its crucial role in the control of viral infections. *Int J Mol Sci* 2022;23:4095.

Supplementary materials
1. Supplementary methods
2. Table 1S – Serial blood counts of patients III-4 and III-7
3. Table 2S – Familial segregation of 3 homozygous variants identified on exome sequencing in the proband III-4

1. **Supplementary methods**

Chromatin fractionation. All steps were performed on ice. Cells were grown in T175 flasks before washing with ice cold PBS and subsequent harvesting by trypsin. A fraction of cells was taken as input control sample and lysed in SNTBS buffer (2% SDS, 1% NP-40, 50 mM Tris pH 7.5, 150 mM NaCl). The remaining cells were lysed in buffer A (10 mM HEPES, 10 mM KCL, 1.5 mM $MgCl_2$, 10% glycerol, 340 mM sucrose, 1 mM dithiothreitol (DTT), 1 mM N-Ethylmaleimide (Sigma-Aldrich, E3876) and protease inhibitor without EDTA (cOmplete™ Mini EDTA-free protease inhibitor cocktail, Sigma-Aldrich, 11836170001). Lysate was supplemented with Triton X-100 to a final concentration of 0.1% and incubated on ice for 8 minutes. After centrifugation at 1300 x g for 5 minutes at 4°C, supernatant and pellet were separated. Supernatant was subsequently centrifuged at 20000 x g and collected as the cytoplasmic fraction. The pellet was washed twice in buffer A and subsequently lysed in buffer B (3 mM EDTA, 0.2 mM EGTA, 1 mM DTT, protease inhibitor without EDTA) on ice for 30 minutes. The lysate was centrifuged at 1700 x g for 5 minutes at 4°C and the supernatant (containing nucleoplasm fraction) and the pellet (containing chromatin) were separated. The chromatin fraction was washed twice in buffer B, lysed in SNTBS buffer and heated to 99°C for 10 minutes.

Peptide digestion and stage tipping. 10 µg of chromatin fraction, lysed in SNTBS, was loaded onto a precast 4-12% Bis-Tris gel (Bold, Thermo Fischer Scientific). Gels were run on 100 V for approximately 3 minutes and subsequently stained by Colloidal Blue staining (Invitrogen LC6025), showing a protein smear of 6 mm. The proteins were excised from the gel in two fractions, a lower and higher molecular weight fraction. The gel slices were subjected to reduction with dithiothreitol, alkylation with iodoacetamide and in-gel trypsin digestion using a Proteineer DP digestion robot (Bruker). Peptides were lyophilized, dissolved in 30 ul/0.1 v/v/v water/formic acid and subsequently analyzed by on-line C18 nanoHPLC MS/MS with a system consisting of an Ultimate3000nano gradient HPLC system (Thermo, Bremen, Germany), and an Exploris480 mass spectrometer (Thermo, Bremen, Germany). For the total lysate samples, cells were grown in T175 flasks and harvested by trypsin. A fraction of cells was taken as input control sample and lysed in SNTBS buffer. The remaining cells were lysed in lysis buffer (8 M Urea in 10 mM HEPES pH 8.0). DTT was added to a final concentration of 10 mM and incubated for 30 minutes at room temperature. The proteins were first digested with 1 µg Lys-C (Lysyl endopeptidase Mass Spectrometry, Fujifilm WAKO pure chemicals corporation) per 50 µg protein for 3 hours at room temperature. The samples were subsequently diluted 4 times in digestion buffer (50 mM ammonium bi-carbonate (NH_4HCO_3, ABC) pH 8.0) and further digested with 1 µg trypsin per 50 µg protein overnight at room temperature in the dark. The reaction was stopped by acidifying the sample to <2.5 pH with 100% trifluoroacetic acid (TFA). The digested peptides were then desalted and concentrated on triple-disc C18 reverse phase Stagetips (Rappsilber et al., 2007)**.** Peptides were retrieved from the stagetips with elution buffer (32.5% acetonitrile and 0.1% formic acid), subsequently vacuum dried, dissolved in 0.1% formic acid and analyzed with an Exploris480 mass spectrometer (Thermo, Bremen, Germany).

LC-MS/MS analysis. The peptide samples were injected (1ul) onto a cartridge precolumn (300 µm × 5 mm, C18 PepMap, 5 um, 100 A, (100/0.1 water/formic acid (FA) v/v) with a flow of 10 ul/min for 3 minutes (Thermo, Bremen, Germany) and eluted via a homemade analytical nano-HPLC column (30 cm × 75 µm; Reprosil-Pur C18-AQ 1.9 um, 120 A (Dr. Maisch, Ammerbuch, Germany). The gradient

was run from 2% to 36% solvent B (20/80/0.1 water/acetonitrile/formic acid (FA) v/v) in 120 min. The nano-HPLC column was drawn to a tip of ~10 µm and acted as the electrospray needle of the MS source. The temperature of the nano-HPLC column was set to 50°C (Sonation GmbH, Biberach, Germany). The mass spectrometer was operated in data-dependent MS/MS mode for a cycle time of 3 seconds, with a HCD collision energy at 30 V and recording of the MS2 spectrum in the orbitrap, with a quadrupole isolation width of 1.2 Da. In the master scan (MS1) the resolution was 120,000, the scan range 400-1500, at an standard AGC target with maximum fill time of 50 ms. A lock mass correction on the background ion m/z=445.12 was used. Precursors were dynamically excluded after n=1 with an exclusion duration of 45 s, and with a precursor range of 10 ppm. Charge states 2-5 were included. For MS2 the scan range mode was set to automated, and the MS2 scan resolution was 30,000 at an normalized AGC target of 100% with a maximum fill time of 60 ms.

MaxQuant peptide search. For the chromatin search, the high and low molecular weight fraction belonging to one replicate were added together in MaxQuant, making it four replicates per group. The peptide search was performed against an in silico digested reference proteome for Homo sapiens obtained from Uniprot.org (September 12th 2022). For digestion Trypsin/P was selected, allowing two missed cleavages. Oxidation (M) and acetyl (protein N-term) were selected as variable modifications while carbamidomethyl (C) was selected as fixed modification, with a maximum of five modifications per peptide. Fast Label Free Quantification (LFQ) was enabled with a minimal ratio count of two, minimum number of neighbours being two and average number of neighbours being six. Match between runs was enabled with a time window of 0.7 minutes to 20 minutes, accepting to match unidentified features. A minimum peptide length of 7 and a maximum of 4600 Da peptide mass was selected. For protein identification, the peptides and razor + unique peptides were set at one.

Antibodies

Antibody name	Source	Host	Catalog number	Dilution used
βTubulin	Cell Signaling Technology	Rabbit monoclonal	2128S	1:1000
Histone H4	Abcam	Rabbit polyclonal	10158-100	1:1000
Histone H2a	Abcam	Rabbit polyclonal	13923	1:1000
Histone H1.2	Abcam	Rabbit polyclonal	17677	1:1000
STAT1	Cell Signaling Technology	Rabbit monoclonal	14994S	1:1000
pSTAT1	Cell Signaling Technology	Rabbit monoclonal	9167S	1:1000
ATP6V1A	Abnova	Mouse monoclonal	H00000523-M02	1:1000
SUMO2/3	University of Iowa	Mouse monoclonal	8A2	1:500
RanBP2	Bethyl	Rabbit polyclonal	A301-796A	1:1000
SENP7	Prof. R. T. Hay Dundee, U.K.	Sheep polyclonal	(Nan Shen et al., 2009)	1:1000

Supplemental material

BMJ Publishing Group Limited (BMJ) disclaims all liability and responsibility arising from any reliance placed on this supplemental material which has been supplied by the author(s)

J Med Genet

Oligonucleotides and plasmid DNA

Name	Source/ sequence	Catalogue number
shRNA SENP7	Sigma-Aldrich Mission® shRNA library	TRC - 004544
shRNA non-targeting	Sigma-Aldrich Mission® shRNA library	SHC002
ABHD1 primers	ABHD1_EX6_F: 5' GAGGCCCAGTCTTCCTTTTT 3' ABHD1_EX6_R: 5' AGTGAGGGGCTGATTGAAGA 3'	
SENP7 primers	SENP7_EX10_F: 5' CCAGTGATGAAGAAGGACCTG 3' SENP7_EX10_R: 5' TTGTCTGAAAATTCAAACTAAGAAAA 3'	
TXNRD1 primers	TXNRD1_EX4_F: 5' TTGCAAGGGAGTCAACAGAG 3' TXNRD1_EX4_R: 5' GTTTGGAGGGTCACATCCAC 3'.	
SENP7 cDNA primers	Exon 1-3 Forward CAAGAGAAAGCTCGGGCGAC Exon 1-3 Reverse TCAGAACGCTGGACTCTCCC Exon 3-4 Forward ACGCTGGACTCTCCCTTTGC Exon 3-4 Reverse TCCGAGGGTGTCCTGTTACT	

Nan Shen, L., Geoffroy, M. C., Jaffray, E. G., & Hay, R. T. (2009). Characterization of SENP7, a SUMO-2/3-specific isopeptidase. *Biochem. J*, *421*, 223–230. https://doi.org/10.1042/BJ20090246

Rappsilber, J., Mann, M., & Ishihama, Y. (2007). Protocol for micro-purification, enrichment, pre-fractionation and storage of peptides for proteomics using StageTips. *Nature Protocols 2007 2:8*, *2*(8), 1896–1906. https://doi.org/10.1038/nprot.2007.261

Tyanova, S., Temu, T., & Cox, J. (2016). The MaxQuant computational platform for mass spectrometry-based shotgun proteomics. *Nature Protocols*, *11*(12), 2301–2319. https://doi.org/10.1038/NPROT.2016.136

Table 1S – Serial blood counts of patients III-4 and III-7

Patients	III-4							III-7		
AGE days	1	3	5	8	9 (GCSF)	10	13	2	52	53
WBC 10^3/µl	5800	3700	3600	3800		8500	16500	7600	9900	5600
Neutrophil abs	0	202	72	76		510	3630	1748	1100	800
%		5.4	2.2	2.1		6.1	22	23%	11.6	13.9
Lymphocytes abs	5104	2997	3168	2166		5355	8085	4180	7600	4760
%	88	81	88	57		63	49	55	77.5	85
Hemoglobin g/dl	21.6	14.5	13.2	12.5		11.2	10.4	15.5	11.5	10.5
Platelets 10^3/µl	310	252	350	265		524	759	317	524	340

Table 2S - Familial segregation of 3 homozygous variants identified on exome sequencing in the proband III-4

Family members	SENP7 c.1474C>T p.Gln492Ter	ABHD1 c.620_623dup p.Val209Thrfs	TXNRD1 c.341T>A p.Leu114Ter
Proband III-4	**HOM**	HOM	HOM
Father II-1	HET	HET	HET
Mother II-2	HET	HET	HET
Sibling III-1	HET	HET	HOM
Sibling III-2	WT	WT	HET
Patient III-3	**HOM**	HET	HET
Father II-3	HET	WT	HET
Mother II-4	HET	WT	HET
Sibling III-5	HET	WT	WT
Sibling III-6	WT	WT	HET
Patient III-7	NA	NA	NA
Sibling III-8	WT	WT	HET
Patient III-9	**HOM**	WT	HET
Sibling III-10	WT	WT	HOM

Supplemental figures

HOM SEQ

HET SEQ

WT SEQ

Figure 1S

Suppl. fig 2S
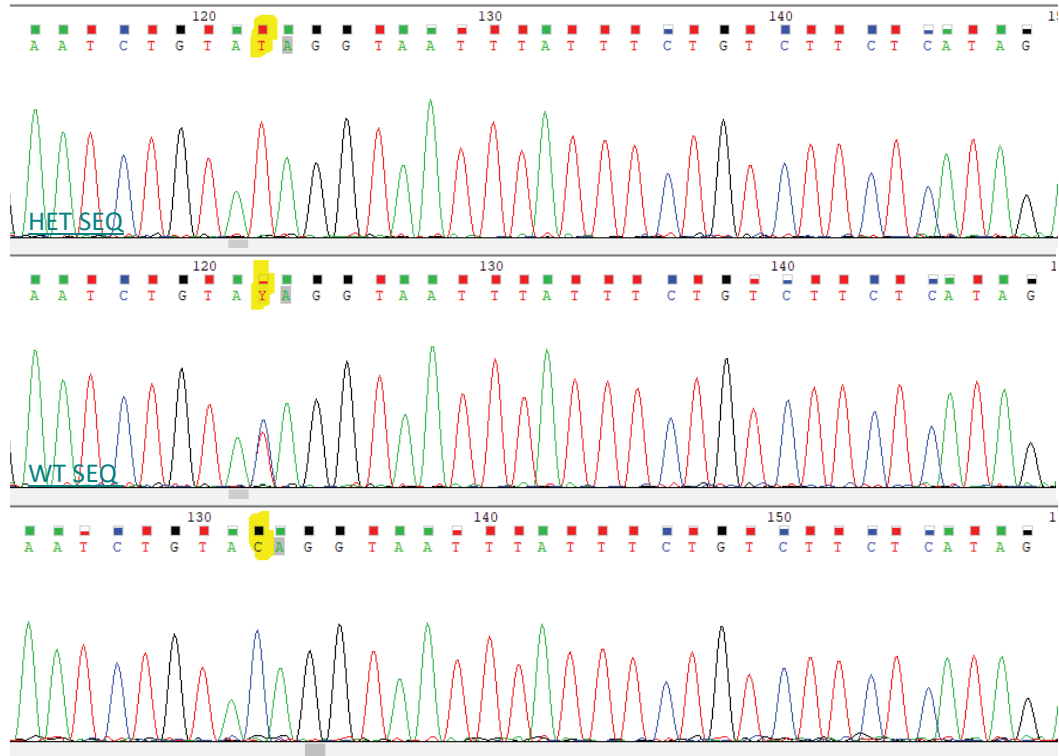
STRING network chromatin fraction
downregulated proteins
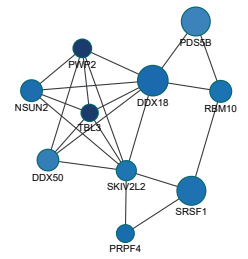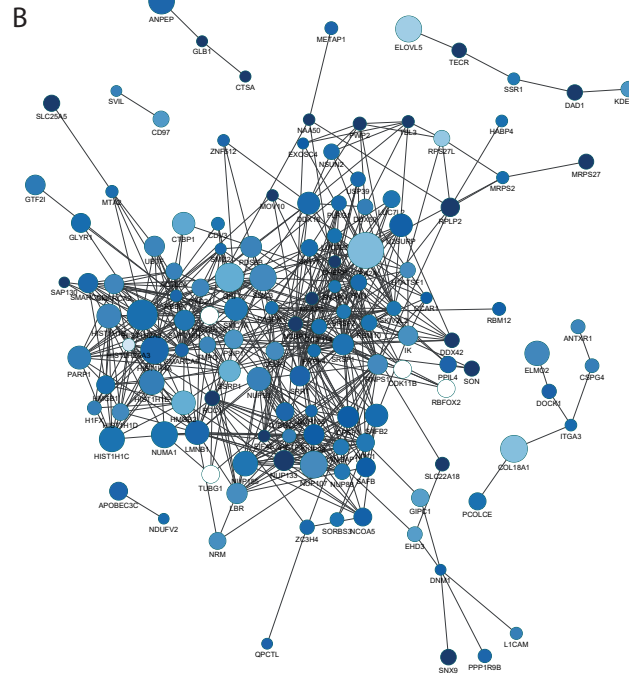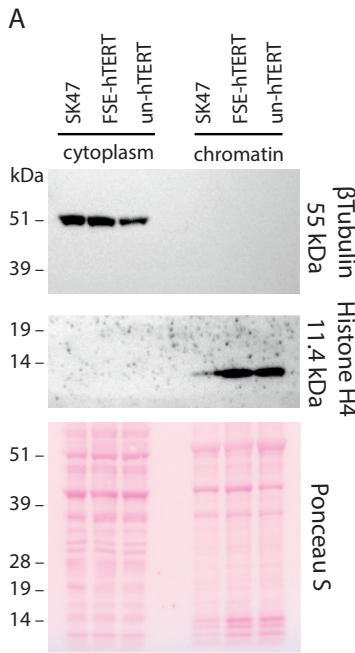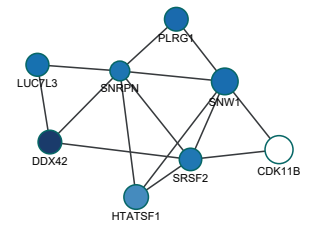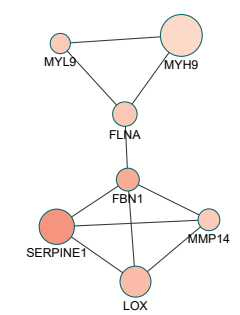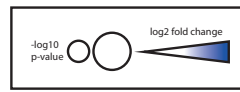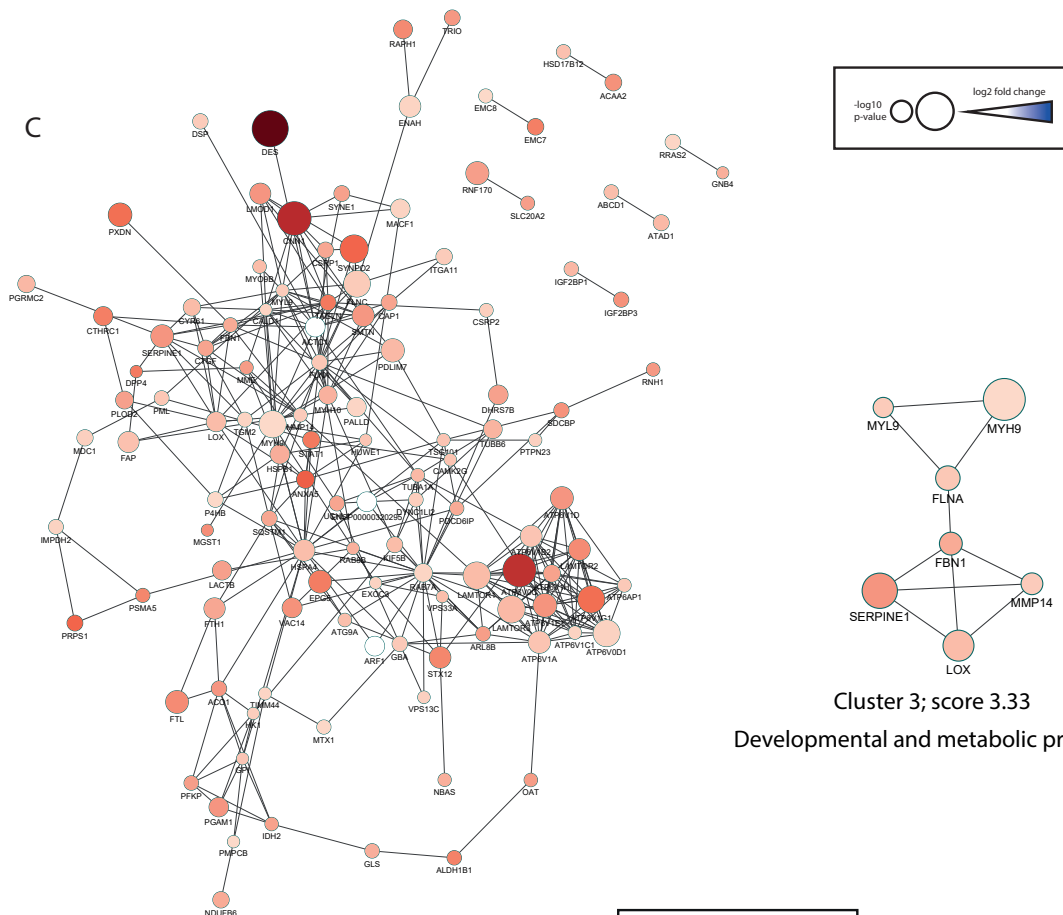
Cluster 3; score 4.7
RNA processing
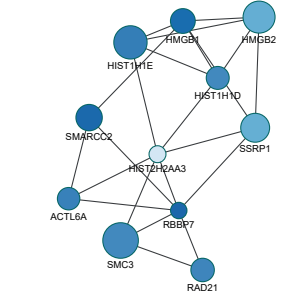
Cluster 4; score 4.4
Chromosome organization

Cluster 5; score 4.0
RNA splicing

STRING network chromatin fraction
upregulated proteins

Cluster 3; score 3.33
Developmental and metabolic process
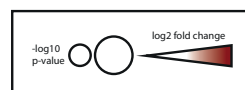
Supplementary figure 2S. Chromatin fractionation experiments. A) Subcellular fractionation was performed and cytoplasmic and chromatin fractions were analyzed by immunoblotting. βTubulin is present in the cytoplasmic fraction, but not in the chromatin fraction. Histone H4 is present in the chromatin fraction but not in cytoplasmic fraction, confirming correct subcellular fractionation. B) STRING network of downregulated proteins in the chromatin fraction of patient cells (indicated in blue). C) STRING network of upregulated proteins in the chromatin fraction of patient cells (indicated in red).

Supplemental material

BMJ Publishing Group Limited (BMJ) disclaims all liability and responsibility arising from any reliance placed on this supplemental material which has been supplied by the author(s)

J Med Genet

Suppl. fig 3S

Supplementary figure 3S. Knockdown of SENP7 in control fibroblasts does not affect histone levels. A) Immunoblots of total cell lysates from patient fibroblasts and control fibroblast, showing lower levels of Histone H4, RANBP2 and HP1α in the patient cells. An increase in pSTAT1 can be seen in patient cells. B) Control fibroblast cells, FSE-hTERT and un-hTERT, were infected with lentiviruses encoding shRNAs against SENP7 or nontargeting control (shControl). Total cell lysates were prepared 72 hours post infection and analyzed by immunoblotting for knockdown efficiency, histone levels (Histone H1.2 and H4), HP1α and STAT1 levels (n = 3). Ponceau S is shown as loading control.